© 2016. Published by The Company of Biologists Ltd | Development (2016) 143, 2780-2790 doi:10.1242/dev.134916

RESEARCH ARTICLE

Live and let die: a REM complex promotes fertilization through synergid cell death in *Arabidopsis*

Marta Adelina Mendes[1,2], Rosalinda Fiorella Guerra[1], Beatrice Castelnovo[1], Yuriria Silva-Velazquez[3], Piero Morandini[1], Silvia Manrique[1], Nadine Baumann[4], Rita Groß-Hardt[4,5], Hugh Dickinson[3] and Lucia Colombo[1,*]

ABSTRACT

Fertilization in flowering plants requires a complex series of coordinated events involving interaction between the male and female gametophyte. We report here molecular data on one of the key events underpinning this process – the death of the receptive synergid cell and the coincident bursting of the pollen tube inside the ovule to release the sperm. We show that two REM transcription factors, VALKYRIE (VAL) and VERDANDI (VDD), both targets of the ovule identity MADS-box complex SEEDSTICK-SEPALLATA3, interact to control the death of the receptive synergid cell. In *vdd-1*/+ mutants and *VAL_RNAi* lines, we find that *GAMETOPHYTIC FACTOR 2* (*GFA2*), which is required for synergid degeneration, is downregulated, whereas expression of *FERONIA* (*FER*) and *MYB98*, which are necessary for pollen tube attraction and perception, remain unaffected. We also demonstrate that the *vdd-1*/+ phenotype can be rescued by expressing *VDD* or *GFA2* in the synergid cells. Taken together, our findings reveal that the death of the receptive synergid cell is essential for maintenance of the following generations, and that a complex comprising VDD and VAL regulates this event.

KEY WORDS: Receptive synergid cell, Pollen tube, Cell death, MADS box, REM, Fertilization

INTRODUCTION

The female gametophyte of flowering plants develops within the ovule and, in many species, including *Arabidopsis thaliana*, comprises a seven-celled structure containing three antipodal cells, two synergid cells, the egg and a central cell (Weterings and Russell, 2004). Cell ablation experiments in *Torenia fournieri* have showed that synergids produce a species-specific signal to attract the pollen tubes (Higashiyama et al., 2006) and at least one viable synergid cell is needed for pollen tube attraction (Higashiyama et al., 2001). In *Arabidopsis thaliana*, the *myb98* mutant has a defective filiform apparatus and consequently fails to attract pollen tubes, confirming a role for the synergid cells in pollen tube attraction (Kasahara et al., 2005). Typically, only one pollen tube penetrates each ovule and delivers two non-motile sperm cells whose release occurs by bursting – an event triggered when the tube interacts with the synergid cell surface (Sandaklie-Nikolova et al., 2007). The receptive synergid cell then degenerates, whereas the other synergid cell remains unaffected.

Hamamura et al. (2011) proposed that it is the loss (through termination of synthesis or degradation) of the pollen tube attractant(s) that results in the inability of the female gametophyte to attract further pollen tubes after a successful fertilization. Fusion of the two sperm cells with the female gametes (egg and central cell) is required to stimulate the degeneration of the second synergid, and the termination of attractant production (Beale et al., 2012; Kasahara et al., 2012). These events have been shown to require both the chromatin-remodeling Polycomb repressive complex 2 (PRC2) (Maruyama et al., 2013) and ethylene signaling (Völz et al., 2013).

Once the pollen tube has interacted with the receptive synergid, its growth becomes arrested. Several gametophytic mutants defective in pollen tube growth arrest have been identified in *Arabidopsis thaliana*, such as *feronia* (*fer*) (Huck et al., 2003), *sirène* (*srn*, allelic to *fer*) (Rotman et al., 2003; Escobar-Restrepo et al., 2007), *lorelei* (*lre*) (Capron et al., 2008 and Tsukamoto et al., 2010), *scylla* (*syl*) (Rotman et al., 2008), *nortia* (*nta*) (Kessler et al., 2010) and *abstinence by mutual consent* (*amc*) (Boisson-Dernier et al., 2008).

Synergid cells have recently been reported to coordinate pollen tube reception and burst via a calcium-mediated response requiring the FER signaling pathway (Ngo et al., 2014). The synergid 'cell-death pathway' is defective in *fer* and *lre* lines, although is not clear whether the receptive synergid, the non-receptive synergid or even both synergids are affected (Ngo et al., 2014). The first unambiguous female gametophytic mutation identified that showed a defective receptive synergid cell death was *gametophytic factor 2* (*gfa2*) (Christensen et al., 2002). GFA2 is a mitochondrial matrix chaperone protein (Christensen et al., 2002), suggesting that synergid cell death in *Arabidopsis* requires functional mitochondria, as already proposed by several authors (see review by Scott and Logan, 2008). A similar situation was also reported for animals, where several studies have demonstrated that functional mitochondria are required both for normal cell growth and division, and for programmed cell death. Paradoxically, most tumor cells, which contain active mitochondria, are resistant to apoptosis (Gogvadze et al., 2008; Wang et al., 2013; Yadav and Chandra, 2014).

VERDANDI (*VDD*), a transcription factor belonging to the reproductive meristem (REM) family (Romanel et al., 2009; Mantegazza et al., 2014), was identified as a target of the ovule identity complex SEEDSTICK-SEPALLATA3 (STK-SEP3) and is required for synergid cell death (Matias-Hernandez et al., 2010). In *vdd-1*/+ ovules, the synergid cells partially lose their identity. They are still able to attract pollen tubes, but never undergo cell death. We

[1]Dipartimento di BioScienze, Università degli Studi di Milano, Milan 20133, Italy. [2]Departamento de Biologia, Faculdade de Ciências, Universidade do Porto, 4169-007 Porto, Portugal. [3]Department of Plant Sciences, University of Oxford, South Parks Road, Oxford OX1 3RB, UK. [4]Center for Plant Molecular Biology (ZMBP), University of Tübingen, 72076 Tübingen, Germany. [5]Center for Biomolecular Interactions Bremen, University of Bremen, Leobener Straße NW2, 28359 Bremen, Germany.

*Author for correspondence (lucia.colombo@unimi.it)

L.C., 0000-0001-8415-1399

Received 7 January 2016; Accepted 2 June 2016

Development (2016) 143, 2780-2790 doi:10.1242/dev.134916

show here that a second REM factor, REM11, is also a target of the STK-SEP3 complex and is involved directly in synergid cell death, together with *VDD*. Since the REM11 mutant exhibited a female phenotype similar to *vdd-1/+*, we decided to follow tradition and name it after a Norse goddess, VALKYRIE (VAL) (from Old Norse valkyrja), who chose those who lived and died in battle (Orchad, 2011). We analyzed the role of VDD and VAL in the context of other genes required for pollen tube-synergid interactions, such as *MYB98*, *FER* and *GFA2*. We found the *vdd-1/+* phenotype is fully rescued by expression of the *VDD* coding sequence in synergid cells using the *MYB98* promoter, and is partially rescued by expressing *GFA2*, suggesting that *GFA2* lies downstream of VDD. Based on these results, we propose an integrated model in which a VDD-VAL complex regulates key events of the fertilization process, including the death of the receptive synergid cell and the death (by bursting) of the pollen tube after growth arrest.

RESULTS

VAL is co-expressed with STK and VDD

Pollen tube reception and synergid cell death are key events in the fertilization process. The female gametophytic phenotype of *vdd-1/+* is important to our understanding of these events because 35% of *vdd-1/+* ovules remain unfertilized even if a viable pollen tube successfully reaches all of them (Matias-Hernandez et al., 2010). To discover further factors involved in this process, we used Affymetrix microarray data from 2000 experiments in a bioinformatics strategy to identify genes with expression patterns similar to *VDD*. The Pearson correlation coefficient (PCC) of individual scatterplots was used to determine the extent of similarity in expression profiles (i.e. co-expression level; for more details, see Materials and Methods). The Affymetrix microarray dataset has proved to be consistent and the calculated PCC values are robust indicators (Menges et al., 2008; Berri et al., 2009). Using this dataset, *STK* and *VDD* show a high degree of correlation (0.812) and emerge amongst the top correlators (see Tables S1 and S2), a group which also includes *SHP1*, *SHP2* and other genes either known to be involved in the process (e.g. *AGO9*; Durán-Figueroa and Vielle-Calzada, 2010) or identified in other screens (*At3g20520*; see Skinner and Gasser, 2009). Nevertheless, *VALKYRIE* (*VAL*) – a gene not previously associated with fertilization – scored the highest PCC value of 0.916 in the Lin analysis for STK (cf. VDD value of 0.798) and was therefore selected for further analysis.

VAL is a direct target of STK-SEP3

As *VAL* presented the highest PCC value, even higher than *VDD* with STK, we performed a sequence analysis of the VAL genomic region searching for putative MADS box binding sites – CArG box sequences. This analysis revealed the presence of two putative CArG box sequences: the first located in the *VAL* promoter region and the second close to the translation start site (Fig. 1A). We performed a chromatin immunoprecipitation (ChIP) assay using STK and SEP3 native antibodies followed by quantitative real-time PCR (qRT-PCR). We also tested SEP3 because it forms a heterodimer with STK, enabling STK to bind DNA (Mendes et al., 2013). qRT-PCR analysis revealed an enrichment of both CArG box regions in the ChIP assays (Fig. 1B). In the anti-STK experiment, chromatin immunoprecipitated from the *stk* single mutant was used as a negative control, whereas in the anti-SEP3 study, wild-type (wt) leaves were used as a negative control, because SEP3 is not expressed in leaves. These results indicate that *VAL*, like *VDD*, is a direct target of the MADS box domain STK-SEP3 protein complex.

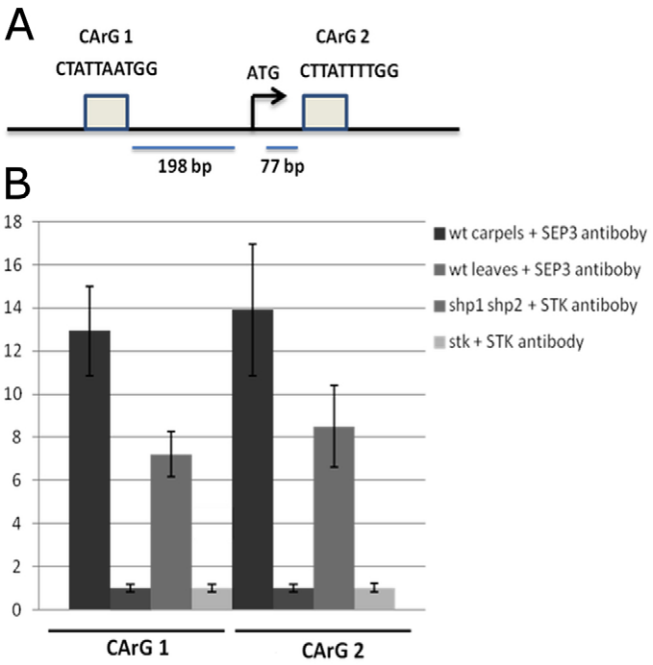

Fig. 1. *VAL* is a direct target of the STK-SEP3 MADs box complex. (A) Schematic representation of the position of CArG boxes in the *VAL* genomic region. (B) ChIP enrichments were validated by qRT-PCR and show that STK and SEP3 are able to bind CArG boxes 1 and 2. The *stk* single mutant was used as a negative control in STK ChIP and wt leaves as a negative control for the SEP3 ChIP assays. *y*-axis shows normalized fold enrichment.

Additionally, *in situ* hybridization experiments were performed to determine *VAL* expression pattern during ovule development. *VAL* is expressed at all stages of ovule development in wt plants (Fig. S1A-F) and high expression was detected in the embryo sac and surrounding layer (Fig. S1E). A higher magnification of the mature ovule demonstrated that a strong signal was present inside the embryo sac in the synergid cell zone (Fig. S1F). Furthermore, the hybridization signal was clearly weaker in *stk* mutant ovules (Fig. S1G) and no expression was observed in *stk shp1 shp2* triple mutant ovules (Fig. S1H). These data confirm that STK, SHP1 and SHP2 redundantly control *VAL* expression in ovules, as is also the case for *VDD* (Matias-Hernandez et al., 2010).

VAL is required for female gametophyte fertility

As no T-DNA insertion lines are available for *VAL* we used an RNA interference approach to investigate the function of *VAL* during ovule development. We obtained 43 transgenic plants containing a *p35S::VAL_RNAi* (*VAL_RNAi*) construct. The immature siliques of these lines were analyzed, and different percentages of unfertilized ovules were observed. We then further divided the transgenic plants into three classes based on the number of unfertilized ovules contained in eight immature siliques per plant. The classes were distributed as follows, comparing always with wt (Fig. 2A): class i, 35% unfertilized ovules (28 plants); class ii, 45% unfertilized ovules (10 plants) (Fig. 2B); class iii, 60% unfertilized ovules (5 plants) (Fig. 2C). Although the siliques contained large numbers of unfertilized ovules, the floral organs developed normally (Fig. 2D). Interestingly, further analysis by qRT-PCR showed the number of unfertilized ovules in the transgenic plants to be proportional to the level of downregulation of the *VAL* transcript (Fig. 2E). *VAL_RNAi* plants with the most severe phenotype had approximately 60% unfertilized ovules and almost complete silencing of *VAL* (Fig. 2E).

Development (2016) 143, 2780-2790 doi:10.1242/dev.134916

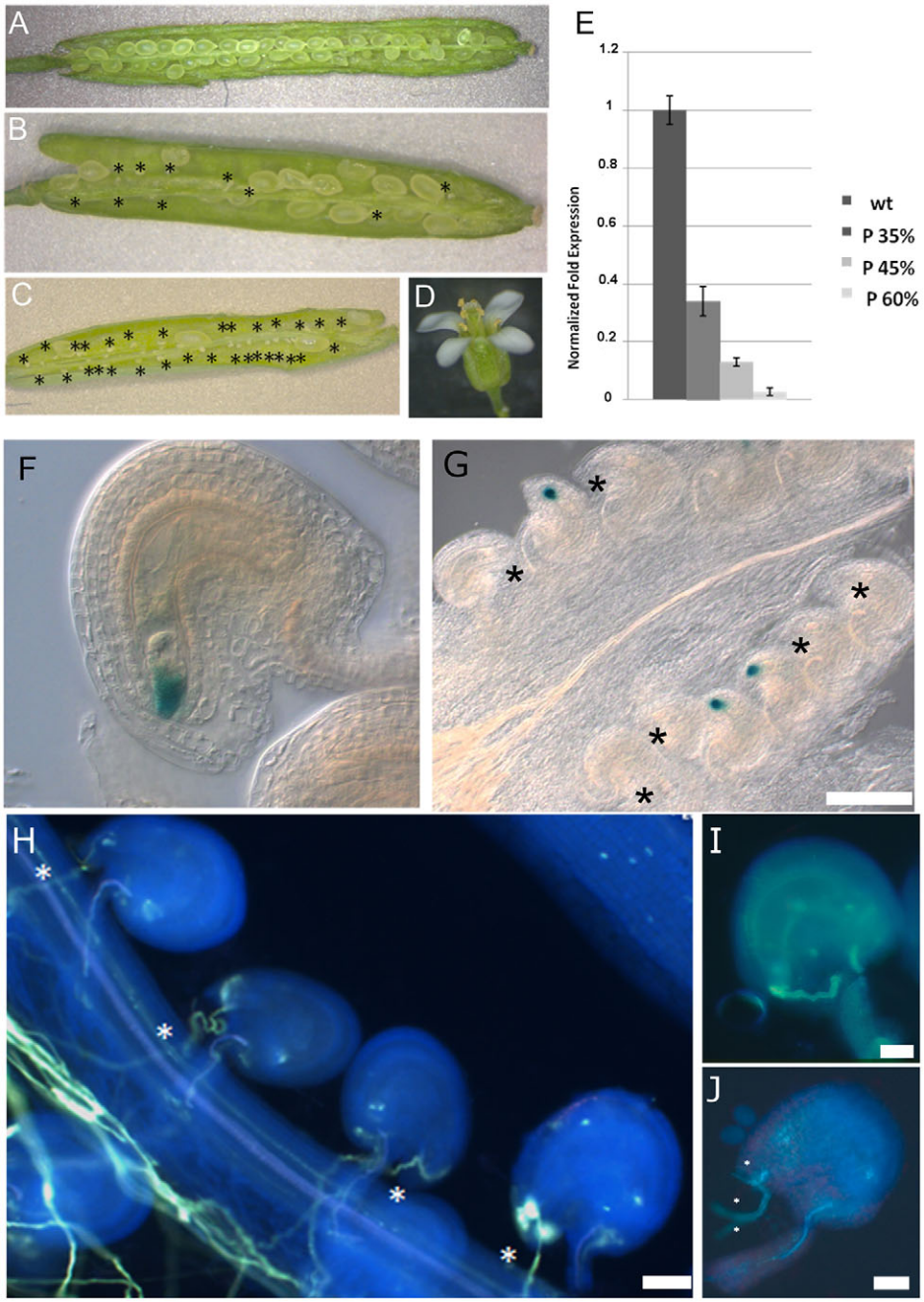

Fig. 2. *VAL_RNAi* plants exhibit a female gametophyte defect. (A) Wild-type silique showing full seed set. (B,C) Siliques of *VAL_RNAi* plants with 45% (B) and 60% (C) unfertilized ovules (black asterisks). (D) Class iii *VAL_RNAi* flower; although the pistil shows 60% unfertilized ovules, all the flower organs are perfectly formed. (E) qRT-PCR in the different *VAL_RNAi* classes. The number of unfertilized ovules perfectly correlates with downregulation of *VAL*. (F) *pCKX7::GUS* in a wt mature ovule. A very strong GUS signal was detected in the synergids region. (G) *pCKX7::GUS* in *VAL_RNAi*. Several mature ovules do not present the GUS signal (asterisks). (H) Aniline Blue staining shows that pollen tubes (asterisks) reach all *VAL_RNAi* mutant ovules 24 h after hand-pollination, even the smaller ovules (unfertilized). (I) Detail of an unfertilized ovule containing a pollen tube. (J) Detail of an unfertilized ovule with two/three pollen tubes (white dots). Scale bars: 50 µm.

To determine whether female, male or both gametophytes were affected by downregulation of *VAL*, we performed reciprocal crosses between *VAL_RNAi* and wt plants. After fertilizing wt plants with pollen from *VAL_RNAi* mutant plants (class iii), only 6% (18/300) of the ovules remained unfertilized , which is similar to the control (equivalent wt crosses, 4.5%; 10/250). Using class iii *VAL_RNAi* plants as female, pollinated with wt pollen, the percentage of unfertilized ovules was 56% (336/600), demonstrating that the reduced fertility phenotype resulted from a female defect.

As in wt plants, the ovules of *VAL_RNAi* plants reached maturity and contained an embryo sac with seven cells (Fig. S2). As the embryo sac seemed to be formed correctly, we further investigated whether ovule sterility resulted from defects in the specification of female gametophytic cell identity. Embryo sac cell-specific reporter constructs were thus introduced into *VAL_RNAi* transgenic lines and gene expression was analyzed in F2 generation, in this way plants were homozygous for the marker. *EC1::GUS* was used as an egg cell identity marker (Sprunck et al., 2012), *FIS2::GUS* as a central cell marker (Chaudhury et al., 1997) and the promoter of the gene *At1g36340* as marker for the antipodal cells (Yu et al., 2005) (Fig. S2). No difference in the GUS marker line expression was detected between *VAL_RNAi* and wt plants, indicating that their cell fates were unaffected by the presence of the transgene. However, analysis of GUS expression using the synergid-specific cell marker line (ET2634; Groß-Hardt et al., 2007) revealed that 277 of 740 (37.5%) embryo sacs to fail to express the synergid specific marker in *VAL* transgenic plants. The percentage of unfertilized ovules per silique (37%) in the transgenic plants corresponded to the number of embryo sacs that failed to show GUS expression in the synergids

Development (2016) 143, 2780-2790 doi:10.1242/dev.134916

(Fig. S2). Köllmer et al. (2014) proposed that the plant hormone cytokinin plays a role in synergid and egg cell development, because *CYTOKININ OXIDASE/DEHYDROGENASE7* (*CKX7*) is strongly expressed in those cells. A similar construct *pCYTOKININ OXIDASE7 (CKX7)::GUS,* but with a nuclear localization signal (NLS) signal to confer a stronger and more specific GUS signal, was used to make crosses with *vdd-1/+* and *VAL_RNAi* (class iii) plants. The GUS expression was strong in the wt synergid cells region (Fig. 2F); plants from the F2 generation homozygous for *pCKX7::GUS* construct showed B-glucuronidase activity in only 72% of *vdd-1/+* ovules (n=600) and in 62% (n=500) of *VAL_RNAi* (class iii) mutant ovules (Fig. 2G).

Synergid cells are responsible for the production of attractant molecules, the guidance cues that ensure each embryo sac (ovule) receives a pollen tube (Higashiyama et al., 2001). We therefore investigated the journey of pollen tubes to the micropyle of mutant ovules. We followed pollen tubes in the transmitting tract using aniline blue staining of the pollen tube walls and found that all ovules of *VAL_RNAi* plants were targeted by at least one pollen tube, indicating that the pollen tube guidance was not affected in this mutant. Importantly, we noticed the ovules investigated fell into two size classes, large (756 of 1200 ovules investigated) having been fertilized within 24 h of pollination, and small (444 of 1200 ovules), remaining unfertilized, although pollen tubes could be seen adjacent to the receptive synergids (Fig. 2G and detail 2H). Furthermore, a low percentage of the ovules (~7% of 444, compared with 2% of 200 in wt; P=0.008, Fisher's exact test) were penetrated by more than one pollen tube (Fig. 2I). Our data thus show that *VAL_RNAi* transgenic lines display a near-identical phenotype to that described for *vdd-1/+* mutants, with both lines showing loss of synergid identity while retaining the ability to attract pollen tubes, (Matias-Hernandez et al., 2010).

The VDD-VAL dimer is required for pollen tube bursting

VDD and VAL proteins belong to the same family, whose members have a putative protein-protein binding domain, and a single protein-DNA binding domain (Romanel et al., 2009; Swaminathan et al., 2008; Mantegazza et al., 2014). The similarity of these mutant phenotypes raised the question as to whether these two proteins were able to interact and form a complex. Using a yeast two-hybrid assay (Y2H), we found clear evidence of an interaction between VDD and VAL (Fig. S3). To explore this interaction *in vivo*, we exploited the bimolecular fluorescence complementation (BiFC) assay to test whether VDD and VAL also interacted *in planta*, using leaves of *N. benthamiana* and basing our assays on the live reconstitution of yellow fluorescence protein (YFP), as previously described by Belda-Palazón et al. (2012). The results confirmed that VDD and VAL were able to fully reconstruct the YFP signal, fused either to the C- or N-terminal fragments of the YFP, forming a heterodimer (Fig. 3A). Furthermore, we discovered that VAL is also able to interact with itself, forming a homodimer (Fig. 3B), whereas VDD alone is not able to reconstitute the YFP signal. We further tested VDD and VAL fused with the C- or N-terminus of the YFP, with empty vectors with the YFP C- or N-terminus as negative controls; no reconstitution of YFP was found (Fig. S3).

To further explore the mechanisms underlying the *vdd-1/+* and *VAL_RNAi* phenotypes, we hand-pollinated both mutants with pollen from plants containing the *Late Anther Tomato52 (pLAT52)::GUS* transgene (Tsukamoto et al., 2010). This marker labels the pollen tube cytosol, allowing the investigation of pollen tube growth and, ultimately, the location of its bursting when in contact with the receptive synergid (Fig. 4A). In wt plants, pollen tube burst was detected in 98% of the 300 ovules analyzed. In the case of the mutant ovules, despite the fact that most of them were reached by at least one pollen tube, only some pollen tubes burst, with other tubes entering the ovule without bursting. Only 71.2% of the 300 *vdd-1/+* ovules analyzed showed pollen tube burst, while the remaining 28.8% stayed in contact with the receptive synergid without any discharge (Fig. 4D). In *VAL_RNAi* pistils, 65% of 250 ovules analyzed showed pollen tube discharge, while the remaining 35% failed to show any bursting (Fig. 4G). These results strongly suggest that both *VDD* and *VAL* are required for pollen tube bursting.

To confirm these results, we used pollen from plants carrying the *HTR10-RFP* transgene, which marks the two sperm nuclei, to visualize the location of the sperm cells in the two mutants and to enable gametic fusion to be monitored (Aw et al., 2010; Hamamura et al., 2011). Importantly, in *vdd-1/+* (Fig. 4E,F) and *VAL_RNAi* (Fig. 4H,I) mutant lines, the two sperm cells arrested in the micropylar area, near to the receptive synergid, at a frequency similar to the number of the unfertilized ovules previously observed in these two mutant backgrounds: 30%

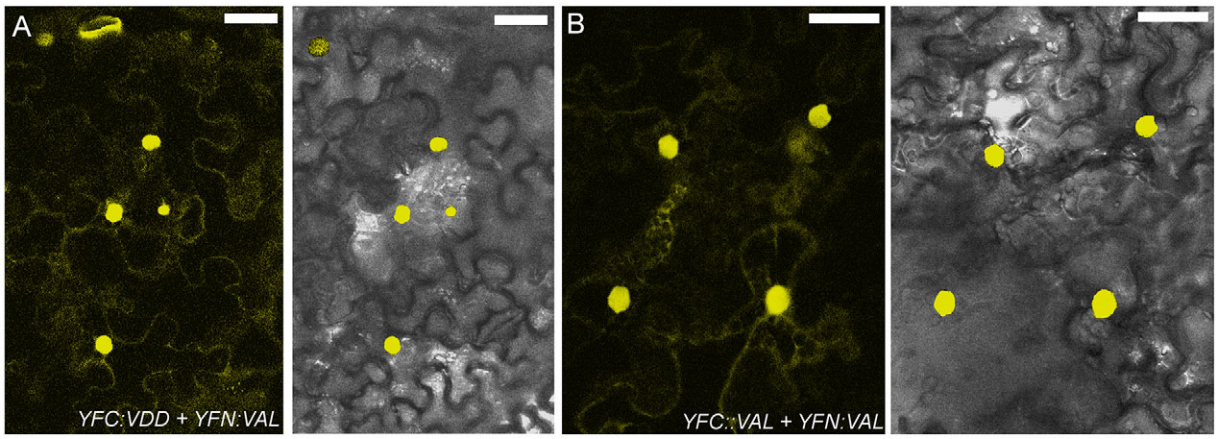

Fig. 3. VDD and VAL interact *in vivo*: BiFC in *N. benthamiana* epidermal leaf cells. BiFC experiments in tobacco leaf cells (A) between transiently expressed VDD and VAL fusions to the C- and N-terminal fragments of YFP, respectively, reconstituting YFP fluorescence (yellow) and (B) between transiently expressed VAL fusions to the C- and N-terminal fragments of YFP, reconstitution of YFP interaction. Negative controls for BiFC experiments are shown in Fig. S4. Right panels in A,B: YFP signal detection; left panels in A,B: overlay of the same section with bright-field image. Scale bars: 50 µm.

Development (2016) 143, 2780-2790 doi:10.1242/dev.134916

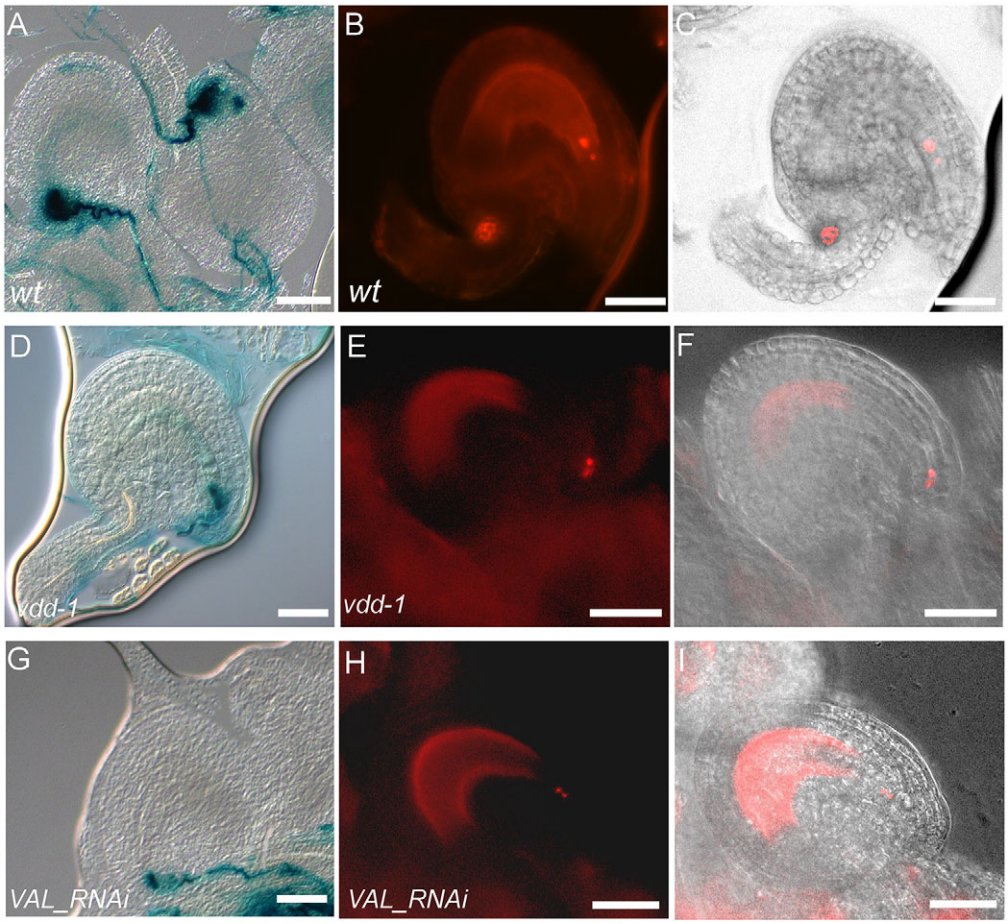

Fig. 4. Pollen tube burst and sperm cell delivery in *vdd-1*/+ and *VAL_RNAi* lines. Pollen tube burst was assessed using *LAT52::GUS* transgene and sperm cell delivery using *HTR10_RFP* transgene. (A) Wild-type ovules, with a clear burst of the pollen tube: a large blue region is seen in the micropylar region. (B) Wild-type ovule showing sperm cell fusion 24 h after pollination. The sperm cells are inside and fusion with the egg and central cell can be observed. (C) Overlay of B with bright-field image. (D) In *vdd-1*/+ ovule, no pollen tube burst was detected. A blue line is visible in the micropylar region very close to the receptive synergid place. (E) Two sperm cells outside the *vdd-1*/+ embryo sac. No fusion was detected with the central or egg cell. (F) In more detail, overlay of E with bright-field image. (G) *VAL_RNAi* ovule, showing no pollen tube burst with *pLAT52::GUS* marker. (H) *VAL_RNAi* ovule with the two sperm cells outside the embryo sac. (I) Overlay with the bright-field image. Percentages of all the crosses are summarized in Table 1. Scale bars: 50 µm.

(*n*=500) of *vdd-1*/+ ovules and 41% (*n*=200) of *VAL_RNAi* ovules.

Structural analysis of mutant embryo sacs – receptive synergid degeneration

To investigate in detail the degeneration of the receptive synergid and the integrity of 'unfertilized' embryo sacs, we carried out confocal laser scanning (CLS) and transmission electron microscopy (TEM) on *vdd-1*/+ and *VAL_RNAi* ovules, from 16 until 48 h after hand-pollination.

As a control for our CLS microscopic analysis, we examined the status of the synergid cells in wt embryo sacs, before and after pollen tube arrival in unpollinated pistils and in hand-pollinated pistils (16 h post pollination). As expected, the two synergids appeared intact prior to pollen tube arrival in the unpollinated pistils (Fig. 5A) and one synergid degenerated after pollen tube arrival (16 h post pollination) (Fig. 5B, detail in C), with the other remaining intact, as described elsewhere.

Both egg and central cells were still clearly visible in *vdd-1*/+ ovules 48 h after hand-pollination (Fig. 5D), revealing that fertilization had not occurred. Importantly, in 16% of the analyzed ovules (Fig. 5E; 16% of *n*=150, unfertilized ovules=32%) two intact synergid cells could be seen, albeit in a different confocal plane from the egg and central cells. The two synergids also remained intact after 48 h in *VAL_RNAi* plants (Fig. 5F; 22% of *n*=160, unfertilized ovules=42%). Developing endosperm could clearly be seen in ovules within the same ovaries that had been fertilized (Fig. 5G).

TEM analysis was used to investigate finer structural details of the embryo sac cells. In *vdd-1*/+ and *VAL_RNAi* lines, those ovules in which the female gametophyte remained unfertilized regularly featured intact egg and central cells (Fig. S4). While these embryo sacs contained two intact synergid cells with classical filiform apparatus (*vdd-1*/+, Fig. 5H,I; *VAL_RNAi*, Fig. 5J), remains of pollen tubes could be detected (recognisable by a high density of organelles, as described by Sandaklie-Nikolova et al., 2007) in the micropylar region. Although the pollen tube had penetrated the ovule and approached the receptive synergid cell in these ovules, neither the pollen tube nor the receptive synergid had degenerated. Further, the synergids presented entirely normal cytology, with intact membranes and key organelles located correctly.

The molecular network controlling synergid cells and pollen tube interaction

The VAL-VDD heterodimer is required for the death of the receptive synergid and consequentially for pollen tube disintegration, but it is clearly not required for pollen tube attraction, suggesting that two or more independent molecular networks may operate in the synergid. MYB98 has been identified as one of the transcription factors responsible for pollen tube attraction to the synergids and we therefore analyzed crosses between the *vdd*/+, and 'class iii' *VAL_RNAi* plants and the marker line *pMYB98::GFP*. In the F2 from this cross, where the transgene was in a homozygous situation, 15 independent plants were analyzed for each mutant. *pMYB98::GFP* was found to be expressed in the two mutant backgrounds (*vdd-1*/+: 97% of 1500 ovules; *VAL_RNAi*: 98% of 800 ovules) as in wt plants (98% of 300 ovules) (Fig. 6A-C), confirming our previous data indicating that pollen tube attraction was not compromised in these mutants.

Development (2016) 143, 2780-2790 doi:10.1242/dev.134916

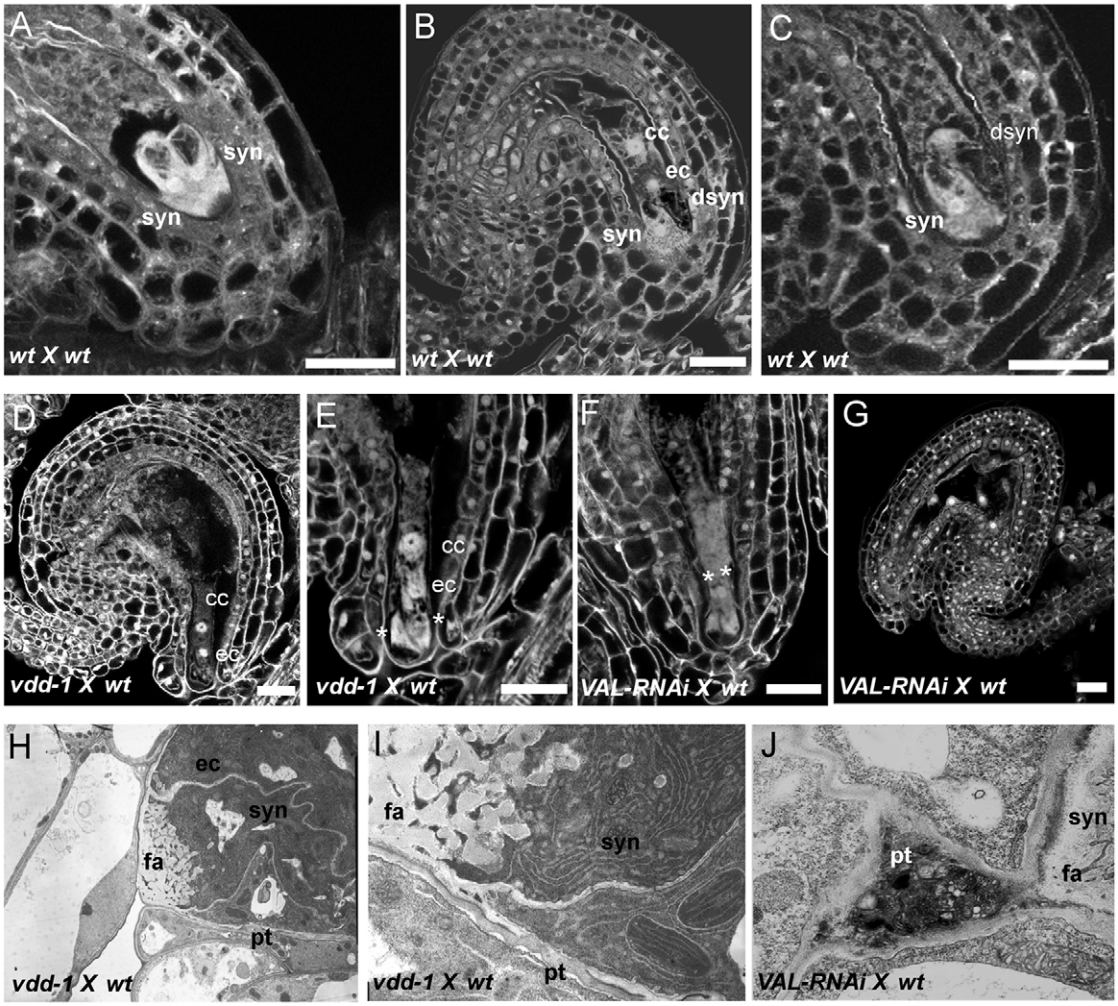

Fig. 5. Confocal and TEM analysis of *vdd-1*/+ and *VAL_RNAi* female gametophytes 48 h after hand-pollination. CLS imaging of (A) wt unfertilized embryo sac and (B) wt fertilized embryo sac, 16 h after hand-pollination. (C) Detail of B. (D) *vdd-1*/+ unfertilized embryo sac 48 h after hand-pollination. The egg cell and central cell are clearly visible and two dark points in the synergid area correspond to two sperm cells. (E) Detail of synergids (asterisk) in a different confocal plane with respect to D. (F) Detail of synergids in *VAL_RNAi* unfertilized embryo sac 48 h after hand-pollination (asterisks). (G) Example of a fertilized ovule 48 h after hand-pollination in *VAL_RNAi*. (H-J) TEM imaging. (H) Transverse section of *vdd-1*/+ gametophyte showing a synergid cell with a pollen tube close by. (I) High magnification of the pollen tube and synergid cell in contact with each other. (J) Longitudinal section of a *VAL_RNAi* ovule showing the interface between pollen tube and filiform apparatus of the synergid cell. dsy, degenerated synergid; syn, synergid; ec, egg cell; cc, central cell; pt, pollen tube; fa, filiform apparatus. Scale bars: 10 µm.

Following attraction to the receptive synergid, growth of the pollen tube is arrested. The receptor like-kinase FERONIA has been proposed to play a key role in this process (Huck et al., 2003) and more recently in the coordination of the Ca^{2+} response during cell death (Ngo et al., 2014). We therefore crossed *vdd-1*/+ and class iii *VAL_RNAi* with *pFER::FER_GFP*, but failed to detect any difference in *FER* expression compared with wt levels (Fig. S5, *vdd-1*/+, *n*=50 and *VAL_RNAi*, *n*=50). We also used qRT-PCR to determine *FER* transcript levels in both mutant backgrounds, but here detected a slight upregulation of *FER* transcripts (Fig. 6G,H; **P*<0.05, *t*-test). Despite this slight variation, overall, our data are consistent with the absence of the classical *fer* 'pollen tube overgrowth' phenotype in our mutant lines.

The only mutant described so far as having a phenotype similar to *vdd-1*/+ and *VAL_RNAi* is *GAMETOPHYTIC FACTOR 2 gfa2*/+ (Christensen et al., 2002). We therefore crossed *vdd-1*/+ and 'class iii' *VAL_RNAi* plants with the *pGFA2::GUS* line and again analyzed the F2 generation. The promoter of GFA2 is active in all flower organs including, mature ovules (Fig. 6D) (Christensen et al., 2002). In the *vdd-1*/+ background, GUS was detectable in the ovule (as in wt); however, low levels of GUS activity were detected in *VAL_RNAi* lines, indicating a strong reduction in *pGFA2* promoter activity. Interestingly, GUS signal was not seen in mature ovules, sporophytic and gametophytic tissues, suggesting that *GFA2* (Fig. 6F) is also a target of VAL in sporophytic tissues (*n*=15 plants, 400 ovules). To confirm the downregulation of *GFA2* expression in *vdd-1*/+ heterozygote plants, we used *GFA2*-specific primers to perform qRT-PCR on *vdd-1*/+ mature carpels, comparing the data with results from wt and *VAL_RNAi* (class iii). As shown in Fig. 6G,H, *GFA2* expression is slightly downregulated in *vdd-1*/+ lines, but still significant (*t*-test, *P*<0.01), greatly repressed in *VAL_RNAi* (*t*-test, *P*<0.001) compared with wt pistils, implying that *GFA2* lies downstream of the VDD-VAL complex, an interpretation that is consistent with the *gfa2*/+ phenotype.

VDD is expressed throughout the embryo sac and it is unclear whether the *vdd-1*/+ phenotype is focused solely on the synergid cell, or if other cells in the *vdd-1*/+ embryo sac are involved. Furthermore, we wished to explore the possibility that a reduction in

Development (2016) 143, 2780-2790 doi:10.1242/dev.134916

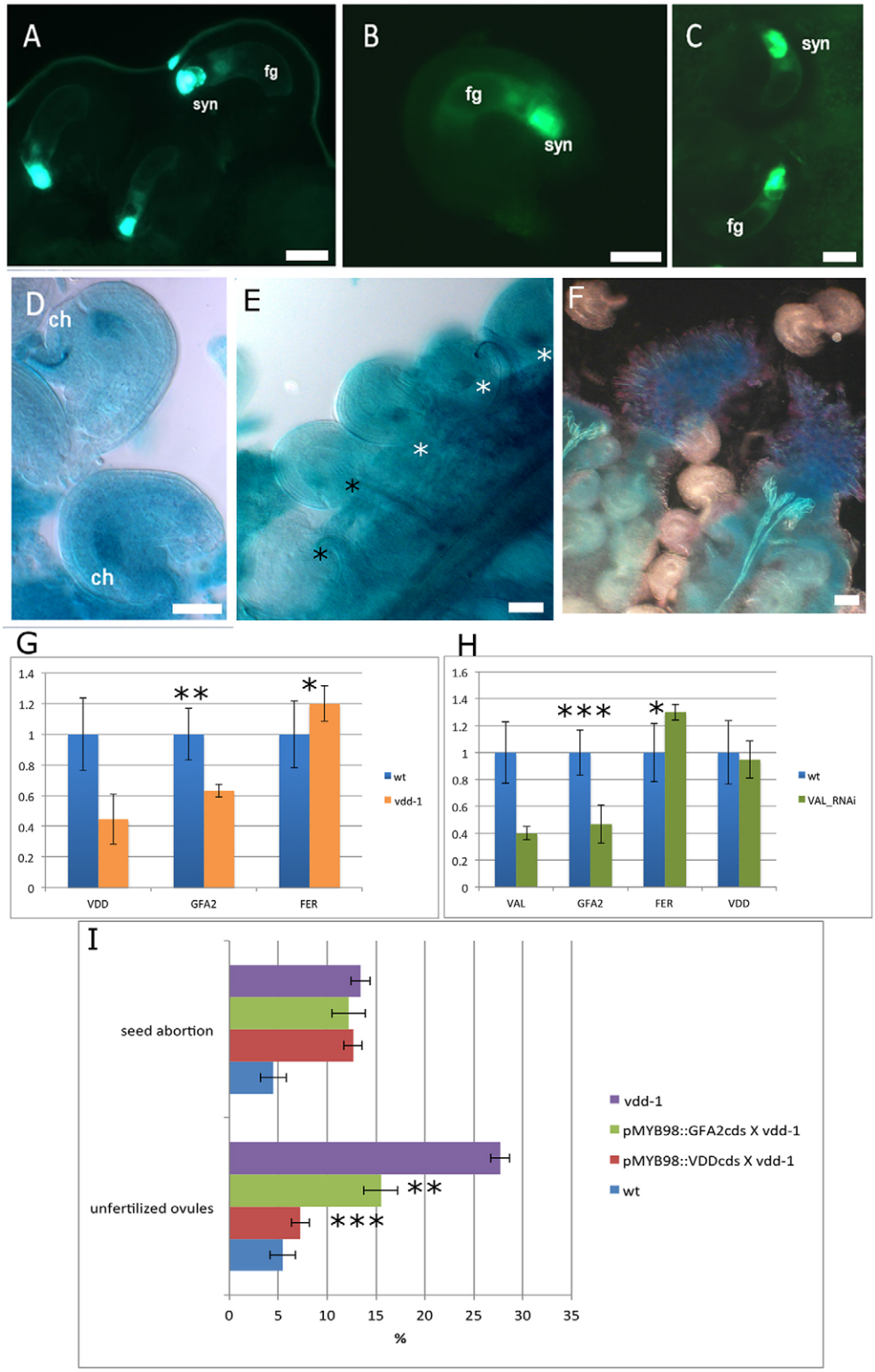

Fig. 6. Molecular network controlling synergid cells and pollen tube interaction in *vdd-1*/+ and *VAL_RNAi* lines. (A) *pMYB98::GFP* in wt mature ovules before fertilization. The GFP signal is confined to the synergids region. In *vdd-1*/+ ovules (B) and *VAL_RNAi* ovules, the GFP signal is equivalent to the wt situation. (D) In wt ovules expressing *pGFA2::GUS*, a pronounced GUS signal is detected in the chalazal zone (ch). (E) In *vdd-1*/+ ovules expressing *pGFA2::GUS*, some ovules have a pronounced blue spot (white asterisks) and some have lost the signal (black asterisks). (F) In *VAL_RNAi* mutant ovules, *pGFA2::GUS* expression was completely lost in all mature ovule tissues. (G,H) qRT-PCR results of *GFA2* and *FER* in *vdd-1*/+ and *VAL_RNAi* mature mutant carpels. Expression of the *VDD* and *VAL* genes was used as a control. (I) Percentages of unfertilized ovules and seed abortion in wt, *vdd-1*/+ mutant, *vdd-1*/+ with *pMYB98::VDDcds* and *vdd-1*/+ with *pMYB98::GFA2cds*. (G,H) **P*<0.05, ***P*<0.01, ****P*<0.001, *t*-test. (I) ***P*<0.04, ****P*<0.0001, *t*-test. Numbers and percentages of the different crosses are summarized in Table 2. syn, synergid; fg, female gametophyte; ch, chalaza. Scale bars: 50 µm.

GFA2 expression resulted in the *vdd* phenotype. Since *MYB98* is active in the mutant background, we used its promoter to drive expression of both *VDD* and *GFA2* coding sequences. Strikingly, as shown in Fig. 6I the *pMYB98::VDD* transgene was able to almost fully complement the *vdd-1*/+ phenotype, reducing unfertilized ovules from 28% to 7% (*t*-test, $P<0.0001$, $n=10$ plants; Fig. 6I). With respect to the role of *GFA2*, the *pMYB98::GFA2* transgene expressed in a *vdd-1*/+ background partially restored the wt phenotype, reducing the number of unfertilized ovules from 28% to 16% (*t*-test, $P<0.04$, $n=8$ plants). In both circumstances, the percentage of seed abortion was maintained (Fig. 6I). These data demonstrate that unfertilized ovules in *vdd-1*/+ lines result from defects in the receptive synergid, and that *GFA2* lies downstream of *VDD* in the pathway regulating these events.

Development (2016) 143, 2780-2790 doi:10.1242/dev.134916

DISCUSSION

Synergid cells are essential for successful fertilization: they are responsible for the attraction, reception and the arrest of the pollen tube, and for preventing entry of other pollen tubes (Beale and Johnson, 2013). We present here structural and molecular data demonstrating that the receptive synergid is also responsible for inducing the bursting of the pollen tube. As proposed by Sandaklie-Nikolova et al. (2007), Ngo et al. (2014) and later, Leydon et al. (2015), our results confirm that cell death of the receptive synergid is coordinated with that of the pollen tube. Furthermore, we show that VDD and VAL, two REM transcription factors and direct targets of the MADS domain complex – STK and SEP3 – are able to interact *in vivo*, indicating that cell death in the receptive synergid requires a complex containing both VDD and VAL, possibly as a heterodimer. Independent disruptions of both VDD (*vdd-1/+*) and VAL (*VAL_RNAi*) exhibit a strong female gametophytic defect, stemming from the absence of the degeneration of the receptive synergid and pollen tube. Importantly, our data also strongly suggest that VDD-VAL complex-mediated synergid cell death is required for bursting of the pollen tube.

The VDD-VAL dimer clearly does not affect attraction and perception of the pollen tube because our data confirm not only that expression of synergid-expressed genes known to be involved in these events (e.g. *MYB98*) are unaffected in our mutant/RNAi lines, but these plants also fail to display the pollen tube overgrowth phenotype characteristic of *feronia* lines, with *FER* expression remaining unaffected. However, elements of the FER signaling pathway are certainly involved in modulating and coupling synergid-generated calcium signals. Ngo et al. (2014) have demonstrated that FER collaborates with the GPI-anchored LRE (LORELEI) at the synergid cell surface to receive signals from the pollen during its phase of slow growth at the embryo sac entrance and triggers a synergid calcium signaling cascade, resulting in the coordinated death of the pollen tube and the receptive synergid. To determine the position of the VDD-VAL complex in this signaling pathway it is thus important to determine whether calcium signals are generated in *vdd-1/+* and *VAL_RNAi* lines.

Other mutants known to have an overgrowing pollen tube phenotype such as *lre* show increased synergid degeneration 48 h after fertilization, suggesting that physical contact with the pollen tube may trigger synergid cell death (Leydon et al., 2015). In our mutants lines, even 48 h after fertilization, we found both ovules with intact synergids (*vdd* gametophyte) and ovules containing a developing endosperm (*VDD* gametophyte), which demonstrates that even if the pollen tube remains in contact with the synergid for a long period, cell death does not occur. This lack of a synergid response suggests that factors other than physical contact may be required for synergid activation. These may include additional ligand-receptor interactions between the pollen tube and synergid, or hormonal pathways within the synergid, involving enzymes such as cytokinin oxidase/dehydrogenase 7 (CKX7), which is responsible for cytokinin degradation and is strikingly downregulated in *vdd-1/+* and *VAL_RNAi* synergids. TEM imaging further supports this persistence of the two synergids, because two perfect synergid cells could be visualized 48 h after pollination, one seemingly in contact a with pollen tube. A low level of 'polytubey' (7% of unfertilized ovules) occurs in *VAL_RNAi* lines, which has also been proposed as evidence of synergid integrity (Beale et al., 2012).

The mitochondrial chaperone *GFA2* (Christensen et al., 2002) is required for synergid degeneration. Leydon et al. (2015) recently showed that *pLAT52::GUS* pollen tubes failed to burst in the *gfa2/+* mutant, a phenotype identical to that of out mutant/RNAi lines. Together with our data showing that GFA2 is downregulated in *VAL_RNAi* and *vdd/+* plants, this result reinforces the view that GFA2 lies downstream of VDD and VAL. Further evidence for GFA2 being both essential for synergid cell death, and regulated by VDD (and probably VAL) is provided by our data showing that a construct containing the *GFA2* coding region under the control of the *MYB98* promoter partially complements the *vdd-1/+* mutant phenotype. The data also demonstrate that the *vdd-1/+* 'unfertilized' ovules phenotype can be complemented using the *VDD* coding sequence under the control of *MYB98* promoter, which is only active in the synergid cells before fertilization, demonstrating that the *vdd-1/+* phenotype is synergid specific. In the future, it will be interesting to investigate whether MYB98 is involved in directly or indirectly modulating *VDD* expression.

Unequivocal evidence is now accumulating that receptive synergid cell death results from a complex exchange of signals between the pollen tube and the synergid. We show here that the receptive synergid controls both pollen tube bursting and its own degeneration and that the VDD-VAL dimer constitutes an essential component of the signaling pathway regulating these events. Based on our findings and those of others, we propose a model (Fig. 7) to explain this crosstalk between female and male gametophytes. The model reflects the independence of diverse pathways and comprises

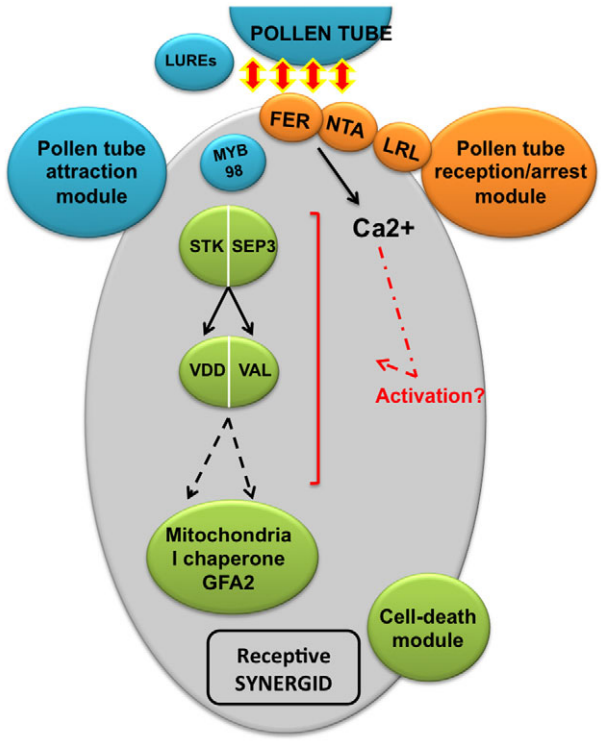

Fig. 7. Model for the control of pollen tube attraction, reception (arrest) and death by the receptive synergid in *Arabidopsis thaliana*. The 'pollen tube attraction module' constitutes the LUREs produced by the synergids that attract the pollen tubes; the transcription factor MYB98 appears to control pollen tube guidance during this event. The 'pollen tube reception and pollen tube arrest module' involves expression of FER, NTA and LRE in the synergid cells, required for pollen tube arrest. The 'cell death module' comprises the STK-SEP3 MADS domain complex that directly regulates the expression of *VAL* and *VDD*, which encode the VAL-VDD dimer that controls expression of the mitochondrial chaperone *GFA2*, which is, in turn, required for synergid cell death and consequently for pollen tube cell death (burst). Ca^{2+} signaling is also involved in the process.

Development (2016) 143, 2780-2790 doi:10.1242/dev.134916

Table 1. Number and percentage of crosses showing pollen tube burst and sperm cell delivery in *vdd_1*/+ and *VAL*_RNAi lines

	PT burst		No PT burst	
Cross (female×male)	*N*	Percentage	*N*	Percentage
wt×*pLAT52::GUS*	294	98	6	2
vdd_1/+×*pLAT52::GUS*	213	71	87	29
VAL_RNAi×*pLAT52::GUS*	195	65	105	35
	Sperm cells in embryo sac		Sperm cells in micropyle	
wt×*HTR10_RFP*	288	96	12	4
vdd_1/+×*HTR10_RFP*	350	70	150	30
VAL_RNAi×*HTR10_RFP*	118	59	82	41

three interacting modules, regulating pollen tube attraction (MYB98, LUREs), pollen tube reception (FER, LRL, NTA) and pollen tube/synergid cell death (VDD, VAL).

Interestingly, in the *stk*, *shp1*, *shp2* triple mutant with one of the alleles heterozygous (e.g. *stk/STK*, *shp1*, *shp2*) the gametophytic defects as described in this study were never observed. Still, we show here convincing evidence that these MADS domain factors are necessary for *VDD* and *VAL* expression in the female gametophyte and for proper synergid function. The most likely explanation is that accumulation of the MADS domain factors in the sporophyte during early stages of ovule development are still available later in the gametophyte cells that derive from the sporophyte to control *VDD* and *VAL* expression.

MATERIALS AND METHODS

Plant material and growth conditions

All plants (*Arabidopsis thaliana*, ecotype Columbia-0, mutants and embryo sac marker lines) were grown at 22°C, under short day (8 h light:16 h dark) or long day (16 h light: 8 h dark) conditions. The *Arabidopsis stk* and *stk*, *shp1*, *shp2* mutants were provided by M. Yanofsky (Pinyopich et al., 2003). The transgenic lines: *pGFA2::GUS* and *pMYB98::GFP* were provided by Prof. Gary Drews (Kasahara et al., 2005; Christensen et al., 2002); *HTR10_RFP* was provided by Frederic Berger (Aw et al., 2010); *FER_GFP* by Prof. Ueli Grossniklaus and *LAT52::GUS* by Prof. Ravi Palanivelu.

Statistical analysis

Values for Pearson correlation were calculated as described (Toufighi et al., 2005) for the 'Expression Angler'. For this purpose, a Visual C++ based program was developed (P.M. and L. Mizzi, unpublished) and the correlation values were calculated from data acquired using the ATH1 GeneChip from Affymetrix deposited at the NASC array database (http://affy.arabidopsis.info/link_to_iplant.shtml). Pearson coefficient calculations were log transformed before calculating the correlation value. This method is explained in Menges et al. (2008) in the section entitled 'Global expression correlation analysis'.

Table 2. Number and percentage of the different crosses with and without GFP/GUS signal in the ovules

	Signal in the ovules		No signal in the ovules	
F2 generation	*N*	Percentage	*N*	Percentage
wt×*pMYB98::GFP*	294	98	6	2
vdd_1/+×*pMYB98::GFP*	1459	97	41	3
VAL_RNAi×*pMYB98::GFP*	784	98	16	2
wt×*pGFA2::GUS*	200	100	0	0
vdd_1/+×*pGFA2::GUS*	182	72	68	28
vdd_1/+×*pCKX7::GUS*	432	72	168	28
VAL_RNAi×*pCKX7::GUS*	310	62	190	38

ChIP and quantitative real-time PCR analysis

In the *VAL* genomic region we found two putative CArG boxes, allowing one mismatch. The first (5′-CTATTAATGG-3′) is located 100 bp before the translation starting site, and the second (5′-CTTATTTTGG-3′), 80 bp after. Primers were designed to test enrichment on these CArG boxes. Primer sequences for first CArG box were: 5′-GGGCCTTAGCGATACCTTGG-3′ and 5′-GTGATTTGATCTAAAGGTGTTGGCC-3′; and for the second CArG box: 5′-GAACACAAGAGGTTTTTCACTTCTCTG-3′ and 5′-CCAGATCATCACCGGATTCACTAGG-3′. Real-time PCR assays were performed in order to determine the enrichment of the fragments. The detection was performed in triplicate using the SYBR Green assay (Bio-Rad) and a Bio-Rad C1000 thermal cycler optical system. ChIP-qPCR experiments and relative enrichments were calculated as reported before (Matias-Hernandez et al., 2010).

Generation of *VAL_RNAi* line

To make the *p35::VAL_RNAi* construct, we used the *Arabidopsis* vector pFGC5941 for dsRNA production obtained from ABRC (stock no. CD3-447). For *VAL* a 247 bp fragment of *VAL* cDNA (position 364-611) was amplified by PCR using primers: AtP_2757 (5′-GGGGACAAGTTT-GTACAAAAAAGCAGGCTACATCTGGAAAAACTTGGAT-3′) and AtP_2758 (5′-GGGGACCACTTTGTACAAGAAAGCTGGGTGATC-ATCACCGGATTCACTA-3′). The fragments were amplified using Phusion High-Fidelity DNA Polymerase (New England BioLabs) and purified using the GeneJET Gel Extraction Kit (Thermo Scientific). The amplified fragments were then cloned into vector pDONR207 (Invitrogen) and subsequently in pFGC5941, using the Gateway system (Invitrogen). Next, *Agrobacterium*-mediated transformation of *Arabidopsis* plants was performed using the floral dip method (Clough and Bent, 1998). Transgenic plants were selected with 10 ng/µl BASTA herbicide.

Cytological assays

The following gametophytic cell reporter lines were used: for the egg cell, the *EC1* gene promoter (Sprunck et al., 2012); for synergid cells, the ET2634 marker line (Groß-Hardt et al., 2007) and pMYB98::MYB98-GFP (Kasahara et al., 2005); for the central cell, the promoter of *At1g02580* (Chaudhury et al., 1997) and for antipodal cells, the *At1g36340* promoter (Yu et al., 2005). All marker lines, except *pMYB98::MYB98-GFP*, contained *GUS* as reporter gene.

The *CKX7* promoter reporter line fragment was amplified using primers 5′-AGTGAGGCGCGCCTTTTCTACTGGAACAACACAATTT-TT-3′ and 5′-AGTGATTAATTAATGTGTGATTGTGTGTAAATGCTA-AAT-3′ and cloned into the pGEM-T vector (Promega). The promoter was excised using *Asc*I/*Pac*I and ligated into the binary vector pGIIBar-EC1::NLS_GUS (Völz et al., 2011) in place of the *EC1* promoter.

The reporter lines were then used as female parental and were hand-pollinated with *VAL_RNAi or vdd-1*/+ pollen. Heterozygous plants, from the F1 generation, were self-fertilized and the presence/absence of the *VAL_RNAi* and *vdd-1* mutations in the F2 generation were examined by PCR. GUS staining was performed in order to detect the presence of the marker and the wt expression profile was always used to confirm the correct expression profile. GUS staining on pistils of emasculated flowers, was performed as described in Liljegren et al. (2000). After staining, the samples were incubated in a clearing solution containing chloral hydrate:glycerol:water in 8:1:2 proportion; then the pistils were dissected and observed using a Zeiss Axiophot D1 microscope equipped with differential interference contrast (DIC) optics. Flowers of *VAL_RNAi* plants were collected at different developmental stages. For ovule development analysis, they were cleared, dissected and analyzed as described previously (Matias-Hernandez et al., 2010). Images were captured with an Axiocam MRc5 camera (Zeiss) using Axiovision software (v.4.1).

In situ hybridization analysis

Arabidopsis flowers were collected at different stages, fixed and embedded in paraffin as described by Huijser et al. (1992). Plant tissue sections were probed with a 317 bp digoxigenin-labeled *VAL* antisense RNA probe amplified using primers atp_2759 (5′-ACATCTGGAAAAACTTGGATC-3′) and atp_2760 (5′-GATCATCACCGGATTCACTAG-3′). Hybridization and immunological detection were executed as described previously by

Development (2016) 143, 2780-2790 doi:10.1242/dev.134916

Coen et al. (1990). Plant tissue sections were also hybridized with *VAL* digoxigenin-labelled sense probe as a negative control.

Yeast two-hybrid (Y2H) and bimolecular fluorescence complementation (BiFC)

Full-length *VAL* and *VDD* CDS were amplified from *Arabidopsis* cDNA. Primers including Gateway *attB1* and *attB2* sites were used to amplify the fragments. Primers, 5′-GGGGACAAGTTTGTACAAAAAAGCAGGCTCGATGAACACAAGAGGAAATTACTCTAATG-3′ and 5′-GGGGACCACTTTGTACAAGAAAGCTGGGTGTCATCCGCTGATAATCTTGAC-3′ were used for *VDD* and 5′-GGGGACAAGTTTGTACAAAAAAGCAGGCTCGATGGTGAAAAACAAAGCTTTTTTTG-3′ and 5′-GGGGACCACTTTGTACAAGAAAGCTGGGTGCTATTCTTTGGAGACTTTCACACG-3′ for *VAL*. Fragments were amplified with Phusion High-Fidelity DNA Polymerase (New England BioLabs). The CDS sequence of each gene was cloned into pDONR207 (Invitrogen) and successively in the pGADT7 and pGBKT7 vectors (Clontech) to make a fusion with Gal4 activation (AD) and binding (BD) domains, respectively, for Y2H assay and into vectors pYFPN43 and pYFPC43 (http://www.ibmcp.upv.es/FerrandoLabVectors.php) for BIFC through Gateway recombination (Invitrogen). BIFC was executed as described by Belda-Palazón et al. (2012).

For Y2H assays each bait/prey pair was transformed into the yeast strain α-AH109 (Clontech). As a control for auto-activation and false positives, each bait was also transformed with the empty AD vector into the yeast strain, and each prey with the empty BD vector. The pair (bait/prey) colonies that grew at 28°C on all selective media (−Trp-Leu-Adenine-His and supplemented with increasing concentrations of 1 mM to 2.5 mM 3-amino-1,2,4-triazole), were considered positive.

Pollen tube guidance, reception, burst analysis and sperm cell migration analysis

Experiments of pollen tube guidance, reception and burst were performed as previously described by Mizzotti et al. (2012).

Confocal and TEM analysis

For confocal laser scanning and transmission electron microscopy (TEM), flowers were emasculated and hand pollinated with wt pollen. For confocal laser scanning, 24-48 h after pollination, pistils were fixed as described by Braselton et al. (1996). Samples were then excited using a laser (532 nm) and emission was detected between 570 and 740 nm. A Leica SP5 confocal laser-scanning microscope was used for this analysis. For TEM analysis, pistils were dissected; ovules were then exposed to the fixative solution by cutting away regions of the ovary wall. Material was fixed in a solution of paraformaldehyde/glutaraldehyde as described in Sandaklie-Nikolova et al. (2007).

Expression analysis by quantitative real-time RT-PCR

Quantitative real-time RT-PCR experiments were performed using cDNA obtained from inflorescences. Total RNA was extracted using the Qiagen RNA extraction Kit. Ambion TURBO DNA-free DNase kit was used to eliminate genomic DNA contamination according to the manufacturer's instructions (http://www.ambion.com/). The ImProm-IITM reverse transcription system (Promega) was used to retro-transcribe the treated RNA. Transcripts were detected using a Sybr Green Assay (iQ SYBR Green Supermix; Bio-Rad) using *UBIQUITIN10* (*AT4G05320*) and *ACTIN8* (*AT1G49240*) as a reference genes. Assays were done in in triplicate using a Bio-Rad iCycler iQ Optical System (software v.3.0a). The fold changes were calculated by normalizing the amount of mRNA against housekeeping gene fragments.

Diluted aliquots of the reverse-transcribed cDNAs were used as templates in quantitative PCR reactions containing the iQ SYBR Green Supermix (Bio-Rad). The expression of different genes was analyzed, using the following primers: *VDD* (RT_795, 5′-GGGAAGGTCATGGCAAGTTA-3′; RT_796 5′-CCATCTGCCTCGAATATGGT-3′), *VAL* (RT_1019 5′-GAAAGGCGGTATCTGGATGA-3′; RT_1020 5′-CCTTGACAAAGATGCAACCA-3′), *FER* (RT_853 5′-CTCTCTCCGATTTCATCGCTTAGG-3′; RT_854 5′-GGATCTTGTGTTAACGCTGG-3′), *GFA2* (RT_926 5′-ACGCGGTTCTCAGTGTTACC-3′; RT_927 5′-TGCACATACTGATCCCCAAA-3′), *UBI* (RT_147 5′-CTGTTCACGGAACCCAATTC-3′; RT_148 5′-GGAAAAAGGTCTGACCGACA-3′) and *ACT8* (RT_861 5′-CTCAGGTATTGCAGACCGTATGAG-3′; RT_862 5′-CTGGACCTGCTTCATCATACTCTG-3′).

Complementation construct

To complement the *vdd-1/+* mutant, we generated a modified version of pB2GW7 (Karimi et al., 2002): the 35S promoter was substituted by a 1794 bp fragment of the *MYB98* gene promoter (*pMYB98* forward primer: 5′-CGGAGATAGTGGCTGAGAGGt-3′; *pMYB98* reverse primer: 5′-GTTCTTGATCACGTGTGAAGATG-3′).

VDD and *GFA2* coding sequences were amplified with primers including *attB1* and *attB2* adaptor sites for cloning into pDONR207, and then recombined into pMYB98-pB2GW7 which contains *attR1* and *attR2* Gateway sites. The *VDD* coding sequence was amplified with primers AtP_3781 (5′-GGGGACAAGTTTGTACAAAAAAGCAGGCTCGATGGTGAAAAACAAAGCTTTTTTTG-3′) and AtP_3782 (5′-GGGGACCACTTTGTACAAGAAAGCTGGGTGCTATTCTTTGGAGACTTTCACACG-3′) and *GFA2* with primers AtP_4343 (5′-GGGGACAAGTTTGTACAAAAAAGCAGGCTCCATGGTCCCTTCCAATGGC-3′) and AtP_4344 (5′-GGGGACCACTTTGTACAAGAAAGCTGGGTGTCACTGGGAAGATCCAGTTG-3′).

pMYB98::VDD and *pMYB98::GFA2* constructs were transformed into *vdd-1/+* plants by floral dipping (Clough and Bent, 1998). Transformed plants were selected using BASTA and presence of the construct was assessed by genotyping. Presence of unfertilized ovules was assessed under the stereomicroscope.

Competing interests

The authors declare no competing or financial interests.

Author contributions

M.A.M. designed and performed most of the experiments and wrote the manuscript. R.F.G. designed and employed the RNA interference construct and performed the ChIP experiment. B.C. performed statistical analyses. Y.S.V. performed TEM imaging. P.M. performed the Pearson coefficient analysis. S.M. made the complementation constructs. N.B. and R.G.H. executed the pCKX7::GUS marker line. H.D. designed the TEM experiment and contributed to writing the manuscript. L.C. designed the experiments and wrote the manuscript.

Funding

M.A.M. was supported by fellowships from the Portuguese National Funding Agency for Science, Research and Technology (Fundação para a Ciência e a Tecnologia) [SFRH/BPD/99936/2014], by the European Union Initial Training Network (ITN) SYSFLO 2010-2013, and by a grant from the European Commission, Marie Curie Action 'Networks for Initial Training' - SYSFLO - Training in Systems Biology Applied to Flowering [FP7-PEOPLE-ITN-2008]. L.C. was supported by Ministero dell'Istruzione, dell'Università e della Ricerca MIUR-PRIN 2012.

Data availability

Correlation analysis data for *STK* and *VDD* are available on Figshare at: https://dx.doi.org/10.6084/m9.figshare.3464054.v2 (Table S1) and https://dx.doi.org/10.6084/m9.figshare.3464057.v2 (Table S2).

Supplementary information

Supplementary information available online at
http://dev.biologists.org/lookup/doi/10.1242/dev.134916.supplemental

References

Aw, S. J., Hamamura, Y., Chen, Z., Schnittger, A. and Berger, F. (2010). Sperm entry is sufficient to trigger division of the central cell but the paternal genome is required for endosperm development in Arabidopsis. *Development* **137**, 2683-2690.

Beale, K. M. and Johnson, M. A. (2013). Speed dating, rejection, and finding the perfect mate: advice from flowering plants. *Curr. Opin. Plant Biol.* **16**, 590-597.

Beale, K. M., Leydon, A. R. and Johnson, M. A. (2012). Gamete fusion is required to block multiple pollen tubes from entering an arabidopsis ovule. *Curr. Biol.* **22**, 1090-1094.

Belda-Palazón, B., Ruiz, L., Martí, E., Tárraga, S., Tiburcio, A. F., Culiáñez, F., Farràs, R., Carrasco, P. and Ferrando, A. (2012). Aminopropyltransferases

Development (2016) 143, 2780-2790 doi:10.1242/dev.134916

involved in polyamine biosynthesis localize preferentially in the nucleus of plant cells. *PLoS ONE* **7**, e46907.

Berri, S., Abbruscato, P., Faivre-Rampant, O., Brasileiro, A. C. M., Fumasoni, I., Satoh, K., Kikuchi, S., Mizzi, L., Morandini, P., Pè, M. E. et al. (2009). Characterization of WRKY co-regulatory networks in rice and Arabidopsis. *BMC Plant Biol.* **9**, 120.

Boisson-Dernier, A., Frietsch, S., Kim, T.-H., Dizon, M. B. and Schroeder, J. I. (2008). The Peroxin Loss-of-Function Mutation abstinence by mutual consent Disrupts Male-Female Gametophyte Recognition. *Curr. Biol.* **18**, 63-68.

Braselton, J. P., Wilkinson, M. J. and Clulow, S. A. (1996). Feulgen staining of intact plant tissues for confocal microscopy. *Biotech. Histochem.* **71**, 84-87.

Capron, A., Gourgues, M., Neiva, L. S., Faure, J.-E., Berger, F., Pagnussat, G., Krishnan, A., Alvarez-Mejia, C., Vielle-Calzada, J.-P., Lee, Y.-R. et al. (2008). Maternal control of male-gamete delivery in Arabidopsis involves a putative GPI-anchored protein encoded by the LORELEI gene. *Plant Cell* **20**, 3038-3049.

Chaudhury, A. M., Ming, L., Miller, C., Craig, S., Dennis, E. S. and Peacock, W. J. (1997). Fertilization-independent seed development in Arabidopsis thaliana. *Proc. Natl. Acad. Sci. USA* **94**, 4223-4228.

Christensen, C. A., Gorsich, S. W., Brown, R. H., Jones, L. G., Brown, J., Shaw, J. M. and Drews, G. N. (2002). Mitochondrial GFA2 is required for synergid cell death in Arabidopsis. *Plant Cell* **14**, 2215-2232.

Clough, S. J. and Bent, A. F. (1998). Floral dip: a simplified method for Agrobacterium-mediated transformation of Arabidopsis thaliana. *Plant J.* **16**, 735-743.

Coen, E. S., Romero, J. M., Doyle, S., Elliot, R., Murphy, G. and Carpenter, R. (1990). Floricaula: a homeotic gene required for flower development in Antirrhinum majus. *Cell* **63**, 1311-1322.

Durán-Figueroa, N. and Vielle-Calzada, J.-P. (2010). ARGONAUTE9-dependent silencing of transposable elements in pericentromeric regions of Arabidopsis. *Plant Signal. Behav.* **5**, 1476-1479.

Escobar-Restrepo, J.-M., Huck, N., Kessler, S., Gagliardini, V., Gheyselinck, J., Yang, W.-C. and Grossniklaus, U. (2007). The FERONIA receptor-like kinase mediates male-female interactions during pollen tube reception. *Science* **317**, 656-660.

Gogvadze, V., Orrenius, S. and Zhivotovsky, B. (2008). Mitochondria in cancer cells: what is so special about them? *Trends Cell Biol.* **18**, 165-173.

Groß-Hardt, R., Kägi, C., Baumann, N., Moore, J. M., Baskar, R., Gagliano, W. B., Jürgens, G. and Grossniklaus, U. (2007). LACHESIS restricts gametic cell fate in the female gametophyte of Arabidopsis. *PLoS Biol.* **5**, e47.

Hamamura, Y., Saito, C., Awai, C., Kurihara, D., Miyawaki, A., Nakagawa, T., Kanaoka, M. M., Sasaki, N., Nakano, A., Berger, F. et al. (2011). Live-cell imaging reveals the dynamics of two sperm cells during double fertilization in Arabidopsis thaliana. *Curr. Biol.* **21**, 497-502.

Higashiyama, T., Yabe, S., Sasaki, N., Nishimura, Y., Miyagishima, S.-Y., Kuroiwa, H. and Kuroiwa, T. (2001). Pollen tube attraction by the synergid cell. *Science* **293**, 1480-1483.

Higashiyama, T., Inatsugi, R., Sakamoto, S., Sasaki, N., Mori, T., Kuroiwa, H., Nakada, T., Nozaki, H., Kuroiwa, T. and Nakano, A. (2006). Species preferentiality of the pollen tube attractant derived from the synergid cell of Torenia fournieri. *Plant Physiol.* **142**, 481-491.

Huck, N., Moore, J. M., Federer, M. and Grossniklaus, U. (2003). The Arabidopsis mutant feronia disrupts the female gametophytic control of pollen tube reception. *Development* **130**, 2149-2159.

Huijser, P., Klien, J., Lonnig, W. E., Meijer, H., Saedler, H. and Sommer, H. (1992). Bracteomania, an inflorescence anomaly is caused by the loss of function of the MADS-box gene SQUAMOSA in Antirrhinum majus. *EMBO J.* **11**, 1239-1249.

Karimi, M., Inzé, D. and Depicker, A. (2002). Gateway vectors for Agrobacterium-mediated plant transformation. *Trends Plant Sci.* **7**, 193-195.

Kasahara, R. D., Portereiko, M. F., Sandaklie-Nikolova, L., Rabiger, D. S. and Drews, G. N. (2005). MYB98 is required for pollen tube guidance and synergid cell differentiation in Arabidopsis. *Plant Cell* **17**, 2981-2992.

Kasahara, R. D., Maruyama, D., Hamamura, Y., Sakakibara, T., Twell, D. and Higashiyama, T. (2012). Fertilization recovery after defective sperm cell release in Arabidopsis. *Curr. Biol.* **22**, 1084-1089.

Kessler, S. A., Shimosato-Asano, H., Keinath, N. F., Wuest, S. E., Ingram, G., Panstruga, R. and Grossniklaus, U. (2010). Conserved molecular components for pollen tube reception and fungal invasion. *Science* **330**, 968-971.

Köllmer, I., Novák, O., Strnad, M., Schmülling, T. and Werner, T. (2014). Overexpression of the cytosolic cytokinin oxidase/dehydrogenase (CKX7) from Arabidopsis causes specific changes in root growth and xylem differentiation. *Plant J.* **78**, 359-371.

Leydon, A. R., Tsukamoto, T., Dunatunga, D., Qin, Y., Johnson, M. A. and Palanivelu, R. (2015). Pollen tube discharge completes the process of synergid degeneration that is initiated by pollen tube-synergid interaction in Arabidopsis. *Plant Physiol.* **169**, 485-496.

Liljegren, S. J., Ditta, G. S., Eshed, Y., Savidge, B., Bowman, J. L. and Yanofsky, M. F. (2000). SHATTERPROOF MADS-box genes control seed dispersal in Arabidopsis. *Nature* **404**, 766-770.

Mantegazza, O., Gregis, V., Mendes, M. A., Morandini, P., Alves-Ferreira, M., Patreze, C. M., Nardeli, S. M., Kater, M. M. and Colombo, L. (2014). Analysis of the arabidopsis REM gene family predicts functions during flower development. *Ann. Bot.* **114**, 1507-1515.

Maruyama, D., Hamamura, Y., Takeuchi, H., Susaki, D., Nishimaki, M., Kurihara, D., Kasahara, R. D. and Higashiyama, T. (2013). Independent control by each female gamete prevents the attraction of multiple pollen tubes. *Dev. Cell* **25**, 317-323.

Matias-Hernandez, L., Battaglia, R., Galbiati, F., Rubes, M., Eichenberger, C., Grossniklaus, U., Kater, M. M. and Colombo, L. (2010). VERDANDI is a direct target of the MADS domain ovule identity complex and affects embryo Sac differentiation in Arabidopsis. *Plant Cell* **22**, 1702-1715.

Mendes, M. A., Guerra, R. F., Berns, M. C., Manzo, C., Masiero, S., Finzi, L., Kater, M. M. and Colombo, L. (2013). MADS domain transcription factors mediate short-range DNA looping that is essential for target gene expression in Arabidopsis. *Plant Cell* **25**, 2560-2572.

Menges, M., Dóczi, R., Okrész, L., Morandini, P., Mizzi, L., Soloviev, M., Murray, J. A. and Bögre, L. (2008). Comprehensive gene expression atlas for the Arabidopsis MAP kinase signalling pathways. *New Phytol.* **179**, 643-662.

Mizzotti, C., Mendes, M. A., Caporali, E., Schnittger, A., Kater, M. M., Battaglia, R. and Colombo, L. (2012). The MADS box genes SEEDSTICK and ARABIDOPSIS Bsister play a maternal role in fertilization and seed development. *Plant J.* **70**, 409-420.

Ngo, Q. A., Vogler, H., Lituiev, D. S., Nestorova, A. and Grossniklaus, U. (2014). A calcium dialog mediated by the FERONIA signal transduction pathway controls plant sperm delivery. *Dev. Cell* **29**, 491-500.

Orchad, A. (2011). *The Elder: A Book of Viking Lore*. London: Penguin Classics. (ISBN-978-0-140-43585-6).

Pinyopich, A., Ditta, G. S., Savidge, B., Liljegren, S. J., Baumann, E., Wisman, E. and Yanofsky, M. F. (2003). Assessing the redundancy of MADS-box genes during carpel and ovule development. *Nature* **424**, 85-88.

Romanel, E. A. C., Schrago, C. G., Couñago, R. M., Russo, C. A. M. and Alves-Ferreira, M. (2009). Evolution of the B3 DNA binding superfamily: new insights into REM family gene diversification. *PLoS ONE* **4**, e5791.

Rotman, N., Rozier, F., Boavida, L., Dumas, C., Berger, F. and Faure, J.-E. (2003). Female control of male gamete delivery during fertilization in Arabidopsis thaliana. *Curr. Biol.* **13**, 432-436.

Rotman, N., Gourgues, M., Guitton, A.-E., Faure, J.-E. and Berger, F. (2008). A dialogue between the sirène pathway in synergids and the fertilization independent seed pathway in the central cell controls male gamete release during double fertilization in Arabidopsis. *Mol. Plant* **1**, 659-666.

Sandaklie-Nikolova, L., Palanivelu, R., King, E. J., Copenhaver, G. P. and Drews, G. N. (2007). Synergid cell death in Arabidopsis is triggered following direct interaction with the pollen tube. *Plant Physiol.* **144**, 1753-1762.

Scott, I. and Logan, D. C. (2008). Mitochondria and cell death pathways in plants. *Plant Signal. Behav.* **3**, 475-477.

Skinner, D. J. and Gasser, C. S. (2009). Expression-based discovery of candidate ovule development regulators through transcriptional profiling of ovule mutants. *BMC Plant Biol.* **9**, 29.

Sprunck, S., Rademacher, S., Vogler, F., Gheyselinck, J., Grossniklaus, U. and Dresselhaus, T. (2012). Egg cell-secreted EC1 triggers sperm cell activation during double fertilization. *Science* **338**, 1093-1097.

Swaminathan, K., Peterson, K. and Jack, T. (2008). The plant B3 superfamily. *Trends Plant Sci.* **13**, 647-655.

Toufighi, K., Brady, S. M., Austin, R., Ly, E. and Provart, N. J. (2005). The botany array resource: e-Northerns, expression angling, and promoter analyses. *Plant J.* **43**, 153-163.

Tsukamoto, T., Qin, Y., Huang, Y., Dunatunga, D. and Palanivelu, R. (2010). A role for LORELEI, a putative glycosylphosphatidylinositol-anchored protein, in Arabidopsis thaliana double fertilization and early seed development. *Plant J.* **62**, 571-588.

Völz, R., von Lyncker, L., Baumann, N., Dresselhaus, T., Sprunck, S. and Gross-Hardt, R. (2011). LACHESIS-dependent egg-cell signaling regulates the development of female gametophytic cells. *Development* **139**, 498-502.

Völz, R., Heydlauff, J., Ripper, D., von Lyncker, L. and Groß-Hardt, R. (2013). Ethylene signaling is required for synergid degeneration and the establishment of a pollen tube block. *Dev. Cell* **25**, 310-316.

Wang, X., Peralta, S. and Moraes, C. T. (2013). Mitochondrial alterations during carcinogenesis: a review of metabolic transformation and targets for anticancer treatments. *Adv. Cancer Res.* **119**, 127-160.

Weterings, K. and Russell, S. D. (2004). Experimental analysis of the fertilization process. *Plant Cell* **16**, S107-S118.

Yadav, N. and Chandra, D. (2014). Mitochondrial and postmitochondrial survival signaling in cancer. *Mitochondrion* **16**, 18-25.

Yu, H.-J., Hogan, P. and Sundaresan, V. (2005). Analysis of the female gametophyte transcriptome of Arabidopsis by comparative expression profiling. *Plant Physiol.* **139**, 1853-1869.

Table S1. Correlation analysis of STK vs all genome, p(LIN) and p(LOG). Pearson coef. > 0.6 . Different colours were used to identify the best correlators - genes that present a high coefficient Lin or Log- with STK (table S1) and VDD (table S2). Interestingly 10 out of the best 15 correlators of STK (67%) are among the best 20 correlators of VDD. Table can be accessed on Figshare at https://dx.doi.org/10.6084/m9.figshare.3464054.v2.

Table S2. Correlation analysis of VDD vs all genome, p(LIN) and p(LOG). Pearson coef. > 0.6. Table can be accessed on Figshare at https://dx.doi.org/10.6084/m9.figshare.3464057.v2.

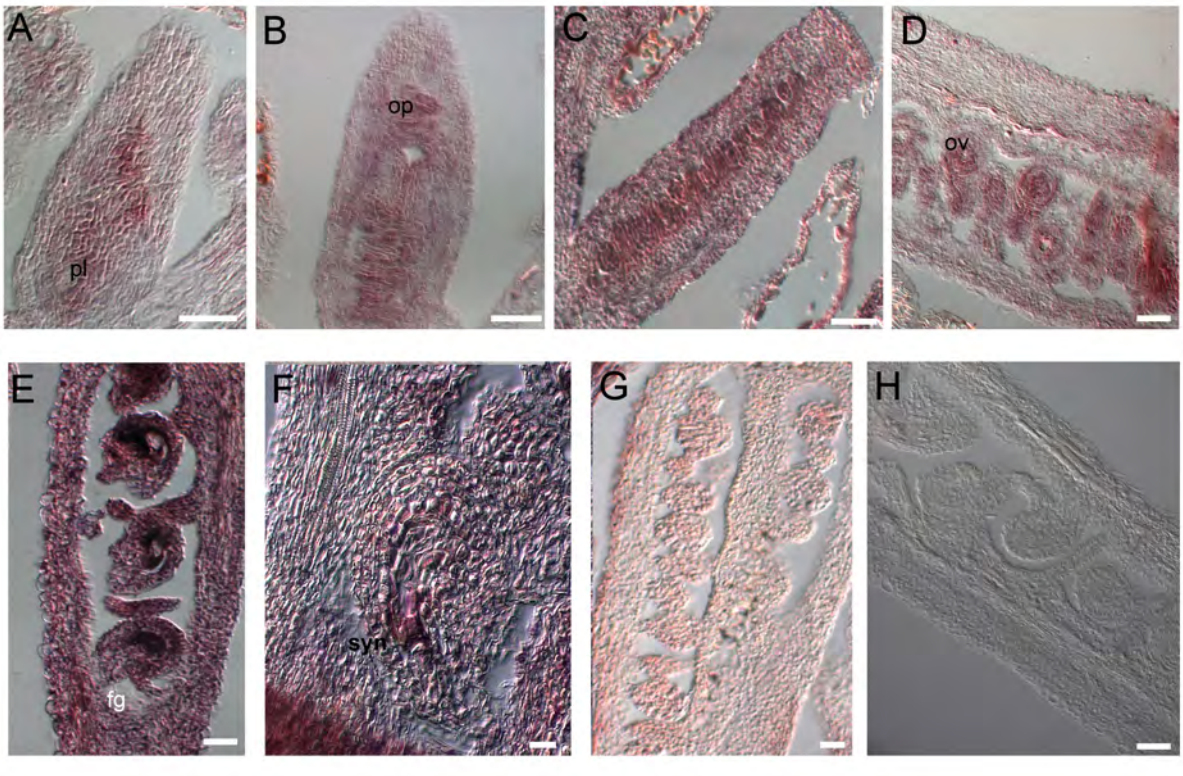

Supplemental Figure 1- *VAL* in situ hybridization

(A-F) *In situ* hybridization experiments performed using wild-type plants: (A-C) *VAL* gene is expressed in the early stages of ovule development; (D) *VAL* mRNA is detectable as a strong signal during later stages of ovule formation; (E) In the mature ovule *VAL* expression is highly detectable inside the embryo sac; (F) mature ovule detail, strong VAL expression inside the embryo sac more precisely in the synergid cells zone (syn). (G) *In situ* hybridization experiment performed in *stk* single mutant, the *VAL* signal is reduced. (H) Experiment performed in *stkshp1shp2* triple mutant background, almost any signal was detected. pl-placenta; op-ovule primordia; ov-ovule; fg-female gametophyte. Scale bars: 50µm.

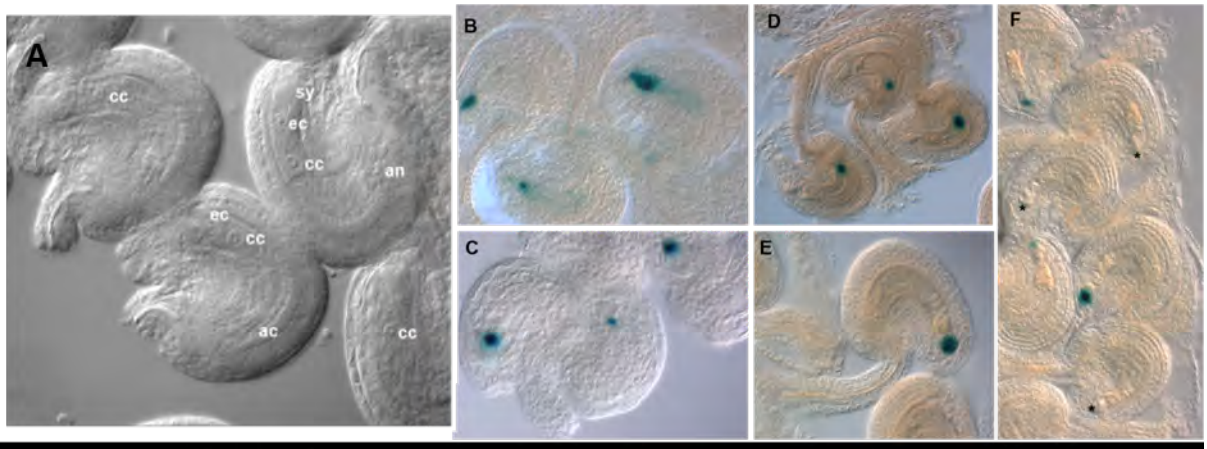

	Genotype	Ovules with signal (%)	Ovules without signal (%)	Unfertilized ovules (%)
Antipodal cells (F2)	wild-type	97%	3%	3%
	VAL_RNAi	92%	8%	30%
Egg cell (F2)	wild-type	95%	5%	4%
	VAL_RNAi	95%	5%	27%
Central cell (F2)	wild-type	98%	2%	2%
	VAL_RNAi	95%	5%	37%
Synergid cells (F2)	wild-type	95% (n=267)	5% (n=16)	2%
	VAL_RNAi	62,5%(n=500)	37,5% (n=300)	37%

Supplemental Figure 2- Embryo sac cells markers in *VAL_RNAi*

(A) Differential interference contrast microscopy (DIC) analysis of *VAL_RNAi* ovules. The ovules are morphologically indistinguishable from the wild type ones, the embryo sac is composed by seven cells. (B-E) Embryo sac cell markers expression in *VAL_RNAi:* (B) egg cell; (C) central central; (D) antypodals and (E-F) synergid cells. The bottom table presents all the percentages and number of ovules analysed. sy- synergids; ec-egg cell; cc- central cell; an- antipodal cells.

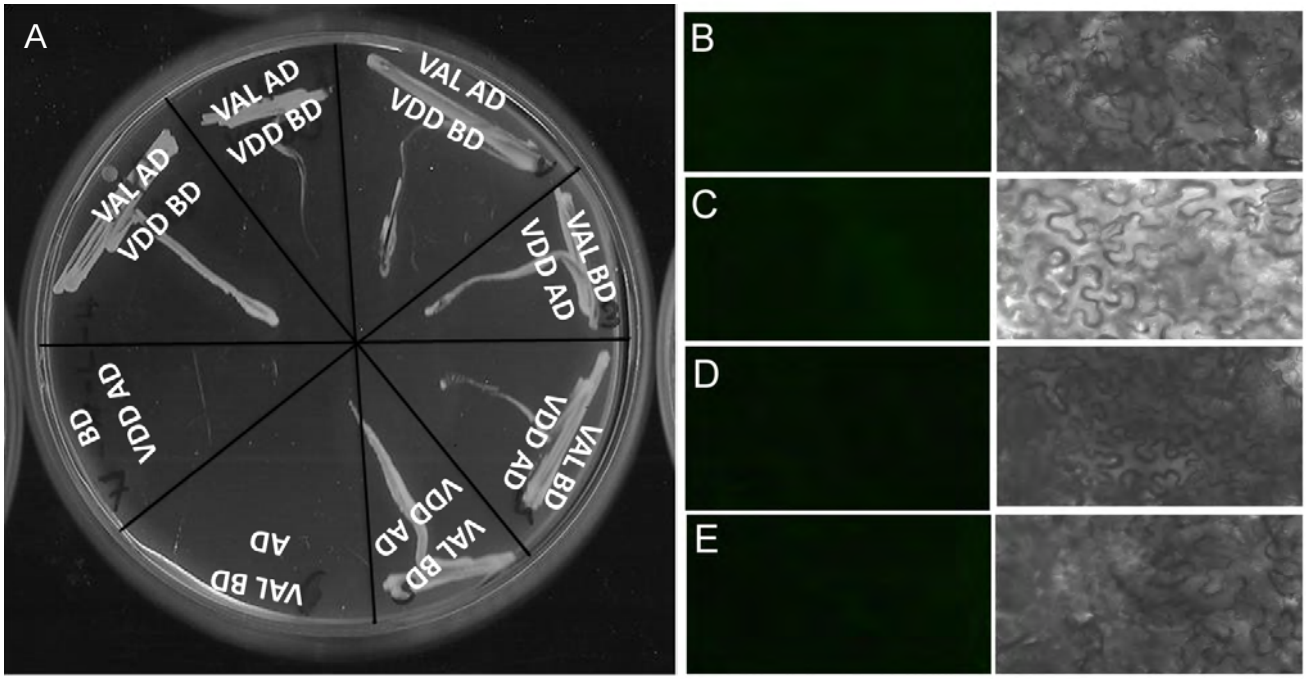

Supplemental Figure 3- Yeast 2 Hybrid (Y2H) experiment and negative BiFC controls

(A) Y2H assay, positive interactions were found for VDD AD versus VAL BD, and vice versa, the colonies growth in -W-L-H + 5mM 3AT selective medium. As negative controls we tested VAL BD vector for empty AD and VDD AD for empty BD vector. (B-E) BIFC negative controls: (B) VDD_YFN plus empty YFC vector; (C) VDD_YFC plus empty YFN vector; (D) VAL_YFN plus empty YFC vector; (E) VAL_YFC plus empty YFN vector.

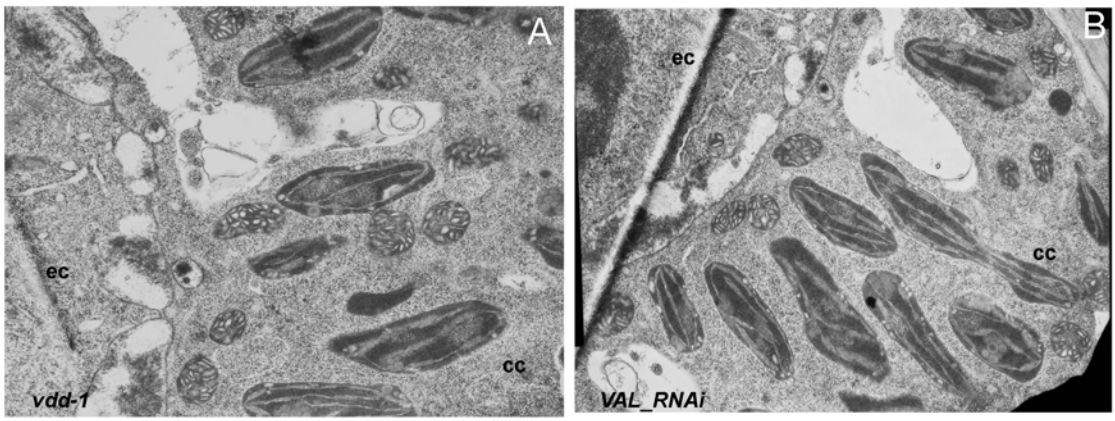

Supplemental Figure 4- TEM imaging of intact egg and central cells in *vdd-1* and *VAL_RNAi*

Those ovules in which the female gametophyte remained unfertilized, regularly featured intact egg and central cells: (A) *vdd-1*; (B) *VAL_RNAi* lines. ec-egg cell, cc- central cell.

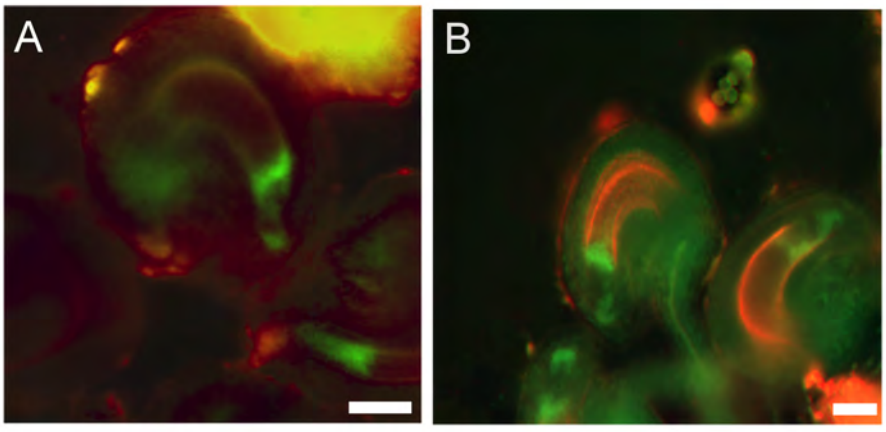

Supplemental Figure 5- *FER_GFP* in *vdd_1* and *VAL_RNAi*

(A) *FER_GFP* in *vdd-1*, *FER* protein localization in the synergids region (n=50 ovules); (B) *FER_GFP* in *VAL_RNAi* background (n=50 ovules). scale bars: 50 µm